PRIMARY RESEARCH ARTICLE

Global Change Biology WILEY

Accelerated shifts in terrestrial life zones under rapid climate change

Paul R. Elsen[1,2] | Earl C. Saxon[3,4] | B. Alexander Simmons[5,6] | Michelle Ward[3,7,8] | Brooke A. Williams[3,8] | Hedley S. Grantham[1] | Salit Kark[9] | Noam Levin[4,10] | Katharina-Victoria Perez-Hammerle[3,11] | April E. Reside[3] | James E. M. Watson[3,8]

[1]Wildlife Conservation Society, Global Conservation Program, Bronx, New York, USA

[2]Department of Forest and Wildlife Ecology, University of Wisconsin-Madison, Madison, Wisconsin, USA

[3]Centre for Biodiversity and Conservation Science, University of Queensland, Brisbane, Queensland, Australia

[4]Department of Geography, The Hebrew University of Jerusalem, Jerusalem, Israel

[5]Global Development Policy Center, Boston University, Boston, Massachusetts, USA

[6]Institute for Future Environments, Queensland University of Technology, Brisbane, Queensland, Australia

[7]WWF Australia, Brisbane, Queensland, Australia

[8]The School of Earth and Environmental Sciences, University of Queensland, Brisbane, Queensland, Australia

[9]The Biodiversity Research Group, The School of Biological Sciences, NESP Threatened Species Recovery Hub, Centre for Biodiversity and Conservation Science, University of Queensland, Brisbane, Queensland, Australia

[10]Remote Sensing Research Centre, School of Earth and Environmental Sciences, University of Queensland, Brisbane, Queensland, Australia

[11]The School of Biological Sciences, University of Queensland, Brisbane, Queensland, Australia

Correspondence
Paul R. Elsen, Wildlife Conservation Society, Global Conservation Program, Bronx, NY 10460, USA.
Email: pelsen@wcs.org

Abstract

Rapid climate change is impacting biodiversity, ecosystem function, and human well-being. Though the magnitude and trajectory of climate change are becoming clearer, our understanding of how these changes reshape terrestrial life zones—distinct biogeographic units characterized by biotemperature, precipitation, and aridity representing broad-scale ecosystem types—is limited. To address this gap, we used high-resolution historical climatologies and climate projections to determine the global distribution of historical (1901–1920), contemporary (1979–2013), and future (2061–2080) life zones. Comparing the historical and contemporary distributions shows that changes from one life zone to another during the 20th century impacted 27 million km^2 (18.3% of land), with consequences for social and ecological systems. Such changes took place in all biomes, most notably in Boreal Forests, Temperate Coniferous Forests, and Tropical Coniferous Forests. Comparing the contemporary and future life zone distributions shows the pace of life zone changes accelerating rapidly in the 21st century. By 2070, such changes would impact an additional 62 million km^2 (42.6% of land) under "business-as-usual" (RCP8.5) emissions scenarios. Accelerated rates of change are observed in hundreds of ecoregions across all biomes except Tropical Coniferous Forests. While only 30 ecoregions (3.5%) had over half of their areas change to a different life zone during the 20th century, by 2070 this number is projected to climb to 111 ecoregions (13.1%) under RCP4.5 and 281 ecoregions (33.2%) under RCP8.5. We identified weak correlations between life zone change and threatened vertebrate richness, levels of vertebrate endemism, cropland extent, and human population densities within ecoregions, illustrating the ubiquitous risks of life zone changes to diverse social–ecological systems. The accelerated pace of life zone changes will increasingly challenge adaptive conservation and sustainable development strategies that incorrectly assume current ecological patterns and livelihood provisioning systems will persist.

KEYWORDS
biodiversity, climate adaptation, conservation, ecosystem change, global change, Holdridge life zones, sustainable development, terrestrial ecoregions

1 | INTRODUCTION

Climatic conditions underpin the distribution of species assemblages, ecosystems, and natural resources across Earth (Kreft & Jetz, 2007; Woodward et al., 2004). Historical climate changes have already impacted all levels of biological organization, from individual genes to entire ecosystems (Scheffers et al., 2016). Changes in temperature alone have been linked to compositional and structural changes in vegetation (Nolan et al., 2018), morphological changes in animals (Sheridan & Bickford, 2011), and alterations to species migration patterns (Miller-Rushing et al., 2008). Such adaptive responses are expected to increase dramatically in the future (Bellard et al., 2012; Pecl et al., 2017). Broad-scale changes in species and ecosystems alter the distribution and availability of natural resources, hindering progress toward sustainable development goals (SDGs) linked to livelihoods, food security, and human health (Adger et al., 2013; Pecl et al., 2017). Climate change also poses a direct challenge for biodiversity conservation given the fluid nature of species ranges yet stationary nature of protected area networks and other recognized conserved areas (Batllori et al., 2017; Elsen et al., 2018, 2020a; Maxwell et al., 2020).

Comparisons of future climate projections with historical climate records have assessed the likely responses of individual species (Lawler et al., 2009) and localized ecosystems (Nolan et al., 2018) to the projected magnitude and trajectory of current climate change (Brown et al., 2020; Burrows et al., 2011; Loarie et al., 2009). Yet our understanding of how climate change impacts broad ecosystem stability is limited. Few global analyses (Neilson et al., 2005; Sisneros et al., 2011) of climate exposure (Loarie et al., 2009) and climate analogs (Williams & Jackson, 2007) go beyond spatial variation in the degree of warming anticipated, to explicitly link climate changes to changes in the distribution of landscape-scale ecosystems based on their sensitivity to climatic conditions (Seddon et al., 2016). A more comprehensive, uniform, and high-resolution approach to translating climate change parameters to landscape-scale ecosystem dynamics is essential for understanding future vulnerability across environmental and socioeconomic sectors because biological (Hanson et al., 2020) and human communities (Smithers & Smit, 1997; Xu et al., 2020) have adapted to—and depend upon—their stable local climate.

We build on previous studies of exposure to climate change (Burrows et al., 2011; Elsen et al., 2020a; Hanson et al., 2020; Loarie et al., 2009; Xu et al., 2020) to quantify the spatial distribution and timing of recent historical and future landscape-scale ecosystem change and stability. We delineate Earth's landscape-scale ecosystems for historical (1901–1920), contemporary (1979–2013), and future (2061–2080) periods at high spatial resolution (1 km^2). We follow the typology of the Holdridge life zones (hereafter "life zones"), a foundational broad ecosystem classification system representing ecologically significant units driven by three climatic parameters: biotemperature, precipitation, and aridity (Holdridge, 1947).

The life zone classification system (Holdridge, 1947) provides a straightforward, intuitive, and sound approach to distinguishing landscape-scale ecosystems and features several important strengths: (i) life zones are dynamic and defined directly from quantitative climate data, without reliance on subjective expert delineation (Olson et al., 2001) or remote sensing (Chen et al., 2015), which are not available for past or future periods; (ii) life zones are based on continuous rather than categorical measures, unlike alternative climate classifications (Beck et al., 2018); (iii) the climatic variables defining life zones directly constrain ecological and ecophysiological processes relevant to the conservation and management of natural resources (Lugo et al., 1999); (iv) life zones have been tested and validated for accuracy, and perform particularly well in forest and tropical landscapes (Pan et al., 2010); and (v) life zones closely align with other broad ecosystem classification systems including land cover, potential vegetation, ecoregions, and the IUCN Global Ecosystem Typology slated for adoption by the Convention on Biological Diversity (CBD) (Keith et al., 2020; Lugo et al., 1999).

It should be noted that the life zone classification system, as an empirical, climatically based model, does not account for physiological or geophysical limits to vegetation growth and thus does not allow for detailed descriptions of vegetative structure and function (Box, 1996). The life zone classification system is an equilibrium model that assumes vegetation responses to climate change are effectively instantaneous. Like other equilibrium and niche models, it ignores both intrinsic and extrinsic factors like reproduction times, dispersal abilities/limitations, natural and anthropogenic disturbances, and geographical barriers to migration that can impact real-world responses and vegetative state transitions (Bergengren et al., 2011; Bond, 2005; Hirota et al., 2011). Nevertheless, it deviates from other models in being defined by combinations of nonlinear climatic gradients to accurately reflect *potential* vegetation, provided that non-climate parameters are compatible. This facilitates an assessment of the degree to which potential vegetation states are projected to persist or shift under climate change globally, and at spatial resolutions relevant for land use policy and ecosystem management. Our approach provides the first high resolution and global assessment of spatiotemporal dynamics among life zones using standardized, empirical, temporally consistent, and ecologically relevant climate information.

We used high-resolution climatologies for temperature and precipitation from historical and contemporary periods (Karger et al., 2017) and a globally consistent model of extraterrestrial solar radiation (Zomer et al., 2008) to quantify the spatial distribution of historical and contemporary life zones (Figure 1a,b). We derived future (2061–2080, midpoint 2070) life zone distributions from the same parameters using a range of downscaled climate projections based on five general circulation models (GCMs) and two representative concentration pathways (RCPs) (Figure 1c). We mapped and tabulated historical and projected future life zone changes within biomes and ecoregions. These nested biogeographic units delineate areas with distinct ecological processes, biodiversity, habitats, and land use patterns (Dinerstein et al., 2017). Consequently, ecoregions have direct relevance to land use policy, as they are a broadly accepted unit by which countries evaluate progress toward SDGs and targets set by the CBD (Convention on Biodiversity (CBD), 2011).
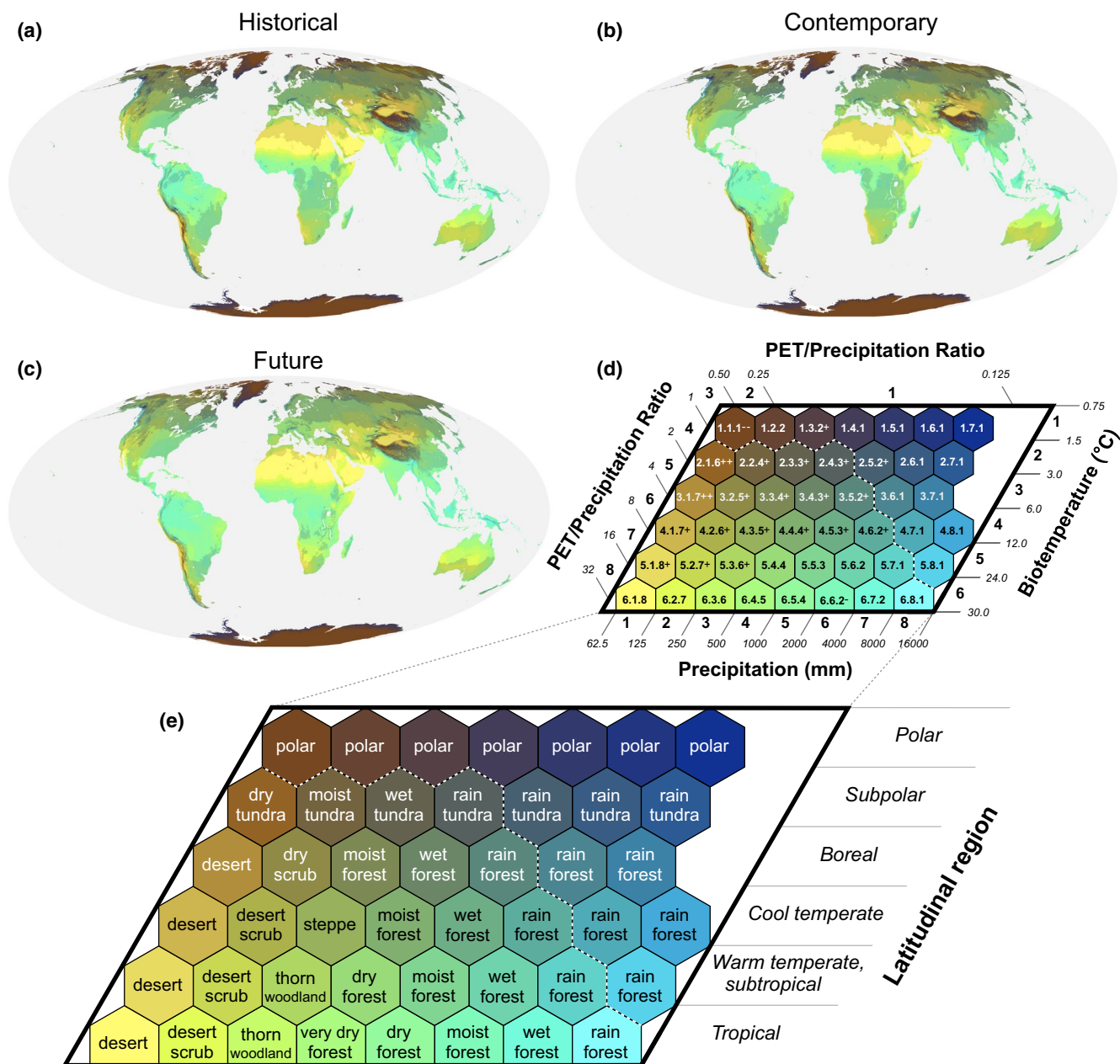
FIGURE 1 Global distributions of (a) historical (1901–1920), (b) contemporary (1979–2013), and (c) future (2061–2080) life zones based on (d) an extension of the Holdridge Life Zone classification system (Holdridge, 1947), as defined by three parameters: biotemperature (six classes), precipitation (eight classes), and aridity, the ratio of potential evapotranspiration (PET) to precipitation (eight classes), along with their descriptions (e). Future life zones are based on an ensemble mean of five general circulation models under RCP8.5. Dashed lines between life zones in (d) and (e) indicate the limits of the 30 original Holdridge Life Zones, while + and − in (d) indicate aridity one class above and below Holdridge (1947), respectively

2 | MATERIALS AND METHODS

2.1 | Holdridge life zones

Holdridge developed the life zone concept as a way to empirically and objectively identify and delineate landscape-scale biogeographic units representing potential vegetation classes, which are based on combinations of three climatic parameters:

biotemperature, precipitation, and aridity (the ratio of potential evapotranspiration, PET, to precipitation) (Holdridge, 1947). In each parameter, the life zones as a whole are constrained at lower and upper bounds set by natural ecological and ecophysiological limits to net primary productivity and water availability. These are 0.75–30°C for biotemperature, 62.5 and 16,000 mm for precipitation, and 0.125 and 32 for a dimensionless index of aridity (Holdridge, 1967). Life zones are delineated along the axes of

biotemperature and precipitation after rescaling to a log$_2$ scale, reflecting the increasing turnover of zones toward the poles and high elevations. The combination of six biotemperature classes and eight precipitation classes results in 48 possible life zones. Holdridge (1947) identified 30 life zones among the 48 possible combinations of six biotemperature classes and eight precipitation classes. While each life zone has a phyto-geographic name, such as "moist forest" (Figure 1e), these describe potential vegetation. Local environmental variation in, for example, slope and soil type, as well as human activities, influence fine-scale vegetation characteristics and the overall condition, land cover, and land use of the landscapes (Lugo et al., 1999).

Holdridge (1947) used the frost line to determine the boundary between warm temperate and subtropical life zones. Subsequent local classifications of life zones used daily minimum air temperature to calculate the average number of frost-free days for this delineation (Lugo et al., 1999). We lumped warm temperate with subtropical life zones because historical and future climate data on frost days were not available.

Though not essential to determining life zone boundaries, Holdridge (1947) included aridity as a third parameter, capturing the ratio of potential evapotranspiration to precipitation. Holdridge (1947) proposed that each life zone occupied one of eight aridity classes in an orderly gradient. The hypothesized association between aridity and life forms in the life zones was considered to be a key constraint, but was never tested by Holdridge, due to the lack of suitable data. We tested Holdridge's predictions by obtaining aridity data for each time period and calculating the mean aridity values for all pixels associated with each life zone (Table S1).

2.2 | Contemporary climate data

We used high-resolution (30 arc-seconds) climatologies of the Earth's land surface area from CHELSA (Karger et al., 2017). CHELSA climate data are based on statistically downscaled model output from the ERA-Interim climatic reanalysis data (Dee et al., 2011). The temperature downscaling process involves regressing temperature lapse rates from ERA-Interim data across a range of atmospheric pressure levels and then interpolating temperatures to sea level using the derived modeled lapse rates. B-spline interpolation is then used to estimate the sea level temperatures between grid cells, and a high-resolution digital elevation model is used to re-project the interpolated temperatures onto the Earth's surface. The precipitation downscaling process incorporates a host of orographic factors and processes, including wind fields, valley exposition, and boundary layer height, and is subsequently bias-corrected through a multistep process. CHELSA data have similar accuracy for temperature estimates when compared with other gridded climatological datasets, but much improved accuracy for precipitation estimates (Karger et al., 2017). Monthly temperature and precipitation climatologies

are available for 1979–2013, which set the bounds for the contemporary period of our analysis.

2.3 | Historical climate data

We used CHELSAcruts time series data (Karger et al., 2017), which provide mean monthly temperatures and total monthly precipitation. The CHELSAcruts algorithm uses the delta change method by B-spline interpolation of anomalies of the CRU TS 4.01 dataset (Harris et al., 2020). For temperature, the interpolated anomalies are added to the high-resolution contemporary CHELSA climatologies; for precipitation, the interpolated anomalies are multiplied by the contemporary climatologies. We used CHELSAcruts monthly data for 1901–1920 to inform the historical period of our analysis. We chose the earliest available data to maximize the duration of its comparison with contemporary data, and chose a two-decade temporal extent to match that available for future climate projections.

2.4 | Future climate data

CHELSA provides downscaled CMIP5 climatologies (downscaled CMIP6 climatologies at 30 arc-second resolution were not yet available) for 2070 (2061–2080) using climatologically aided interpolation based on the contemporary CHELSA climatologies (Karger et al., 2017). Future downscaled climate models are available for several GCMs and multiple RCPs. We selected five GCMs to incorporate model uncertainty, following the recommendation of selecting models with minimum levels of interdependence (Sanderson et al., 2015). We selected CESM1-BGC, MPI-ESM-MR, ACCESS1-3, MIROC5, and CMCC-CM. For each GCM, we considered RCPs 4.5 and 8.5 to evaluate differences between moderate and high radiative forcing scenarios (Hayhoe et al., 2017). Unless otherwise noted, we present the results from an ensemble mean of the five GCMs for RCP8.5 in the main text.

2.5 | Biotemperature

To calculate biotemperature, we calculated the mean among mean annual temperatures in each period (1901–1920, 1979–2013, and 2061–2080). Individual annual means were derived from monthly means for the contemporary and future periods. Monthly mean temperatures were not available for the historical period. Instead, monthly mean temperatures were derived as:

$$(\text{monthly } t_{max} + \text{monthly } t_{min}) \div 2 \qquad (1)$$

In accordance with Holdridge (1947), we replaced all values below 0.75° with 0.75° and all values greater than 30°C with 30°C (Figure S1).

2.6 | Precipitation

We calculated mean annual precipitation by summing the total monthly precipitation for each year in each period. In accordance with Holdridge (1947), we replaced all values below 62.5 mm with 62.5 mm (Figure S1). The maximum observed precipitation did not exceed Holdridge's upper bound of 16,000 mm, so upper bound clamping was unnecessary.

2.7 | Aridity

We used the modified Hargreave's equation (Droogers & Allen, 2002) to calculate monthly PET for each year in each period:

$$\text{PET} = 0.0023 \times r \times (t_{\text{mean}} + 17.8) \times td^2 \qquad (2)$$

where r is the top of atmospheric radiation in mm/month, t_{mean} is monthly mean temperature in °C, and td is temperature range in °C, calculated as annual $t_{\text{max}} - t_{\text{min}}$. For r, we used extraterrestrial solar radiation rasters obtained from the CGIAR Global Aridity and PET Database version 1 (Zomer et al., 2008), converted to monthly values, which matched the spatial resolution (30 arc-seconds) of our other climate parameters. We assumed r to be constant across the three time periods. For td, we calculated the difference of the monthly mean t_{max} and t_{min} for each period. For t_{mean}, we calculated (monthly t_{max} + monthly t_{min}) ÷2 for each period. We then calculated total annual PET for each period by summing all monthly PET layers within each period, and then clamped these layers to a range of 0.125–32, following Holdridge (1947). We calculated aridity by dividing total annual PET by mean total precipitation, as calculated above, for each period (Figure S1). Preprocessing of all life zone climate parameters was done in *R* version 3.6.1.

2.8 | Life zones

Following Holdridge (1947), we $\log_2$-transformed all climate variables to achieve equal intervals for hexagonal bins in life zone parameter space (Figure 1d). We then calculated the centroid value of each life zone hexagonal bin for each climate variable (Sisneros et al., 2011) and $\log_2$-transformed all centroid values to match the scale of the input climate parameters. We assigned each pixel value to the life zone with centroid values nearest to the pixel's observed combination of biotemperature and precipitation values. We repeated this allocation process using historical, contemporary, and future (two RCPs) climate parameters as inputs to produce separate life zone rasters for each period (Elsen et al., 2021). To capture variability across GCMs when calculating future life zones, we took the mean biotemperature, precipitation, and aridity value among all five GCMs within a given RCP prior to the $\log_2$-transform step.

After processing all life zones, we applied a static surface water mask based on a combination of MODIS imagery and the Shuttle Radar Topography Mission (SRTM) Water Body Dataset at 250 m (Carroll et al., 2009) to remove pixels erroneously classified as land (future losses to sea level rise were ignored). We processed all life zones in Google Earth Engine (Gorelick et al., 2017).

2.9 | Life zone area changes

To calculate life zone area changes, we created one raster stack from the historical and contemporary life zone layers, and one raster stack from the contemporary and future life zone layers for each RCP. We then assigned a unique code to each combination of life zones in each transition stack, reflecting each example of life zone stability or change observed in each period. We calculated areas for each stability class and change class and summed the total area of stable or changing life zones. We then summarized these area changes by ecoregions ($n = 847$) and biomes ($n = 14$), using updated delineations from the RESOLVE Ecoregions 2017 dataset in Google Earth Engine (Dinerstein et al., 2017).

To gain insight into how projected life zone area changes might impact current biodiversity, agriculture, and human population patterns, we summarized a set of four metrics related to these parameters within ecoregions (Figure S2). For biodiversity, we calculated range size rarity (also termed "endemism richness," "range rarity richness," and "weighted endemism"; Guerin & Lowe, 2015; Kier et al., 2009), a commonly used metric of endemism calculated as the sum of inverse ranges of all species occurring within a grid cell (i.e., the proportion of a species' range contained within a given pixel), aggregated across all bird, mammal, and amphibian species, and averaged across all pixels within each ecoregion (Kier et al., 2009). We used range size rarity as a metric of endemism (as opposed to alternative metrics, such as corrected weighted endemism; Laffan & Crisp, 2003) because it combines information on both richness and geographic range size to more holistically characterize biodiversity patterns at the global scale. Alternative metrics of endemism are also highly correlated (Guerin et al., 2015), and thus it is unlikely that results will differ substantially using alternative metrics. We also assessed the average number of threatened (IUCN Red List categories CR, EN, and VU) bird, mammal, and amphibian species across all pixels within each ecoregion because we believe this could provide useful information for those species needing urgent conservation attention.

Both biodiversity datasets were derived from IUCN species range maps and produced at 5 km resolution (IUCN, 2021). While biodiversity patterns are inherently scale dependent (Daru et al., 2020), the 5 km resolution is advantageous as it closely matches the 30 arc-second spatial resolution of our climate data and allows patterns to be reasonably summarized at the ecoregion scale.

For agriculture, we used the Global Land Cover-SHARE database (Latham et al., 2014), a harmonized global land cover classification system that provides the proportion of different land cover classes at the pixel level at 30 arc-second spatial resolution, to calculate the percentage of each ecoregion containing cropland. For

human populations, we calculated the population density within each ecoregion using the Gridded Population of the World version 4.11 dataset, which provides population density for the year 2020 at 30 arc-second spatial resolution (CIESIN, 2018). We first converted population densities at the pixel level to population counts by multiplying each pixel value by its area. We then summed all pixel values per ecoregion and divided by its area to calculate its overall population density. For each of these four metrics, we investigated their relationships with the percentage of life zone area change across ecoregions by calculating correlation coefficients and plotting the fits of generalized additive models (GAMs), using cubic regression splines and fitted with restricted maximum likelihood estimation to accommodate potential nonlinear relationships.

2.9.1 | Anomalies

Historical biotemperature values for 103,248.4 km^2 (0.07% of land area) along coasts and inland waters were found to be extremely low, implying improbable changes in biotemperature of three or more classes between historical and contemporary periods. Similar anomalies, covering 27.5 km^2 (0.00002% of land area), occurred in the contemporary dataset (Table S1). We removed these anomalous pixels prior to calculating area changes.

3 | RESULTS

3.1 | Life zones

Of the 48 possible life zones, our analysis confirmed the presence of 45 life zones in historical and contemporary periods (Figure 1; Table S1). This included 15 additional life zones not recorded by Holdridge (1947), which occur in colder and wetter regions of life zone parameter space than the original life zones. These 15 life zones make up approximately 13% of total land area in the historical period, 12% of total land area in the contemporary period, 11% of total land area in 2070 under RCP4.5, and 10.5% of total land area in 2070 under RCP8.5 (Table S1).

We found 26 life zones (58%) fell within the hypothetical aridity class proposed by Holdridge (1947) (Table S1). The predicted values were commonly underestimated by one aridity class (i.e., predicted to be less arid than observed by data). Underestimations occurred most frequently among subpolar, boreal, and cool temperate life zones, infrequently among warm temperate life zones, and only once among tropical life zones (Table S1).

3.2 | Historical life zone changes

Despite recognizable influences of climate change during the 20th century (Root et al., 2003), most land (81.7%) did not change from one life zone to another between historical and contemporary periods (Figures 2 and 3a). However, approximately 26 million km^2 (18.3% of land) did change from one life zone to another, for an average lapse rate of 0.21% per year. Most of these changes were to neighboring warmer or wetter zones as observed in several parts of the boreal biome, the western Amazon and southeastern Brazil, central and east Africa, and central Australia (Figures 2 and 3a). Changes to wetter life zones occurred across large portions of northern Russia, the central Amazon, and southern South America. Changes to distinctly drier life zones occurred in West Africa, parts of the Middle East, and eastern Brazil (Figure 3a).

As expected, boundaries between life zones shifted poleward and toward higher elevations, leading to expansions of zones associated with equatorial climates and contractions of zones associated with temperate climates (Figures 2 and 3a). At midlatitudes, we also observed longitudinal expansions of continental life zones and contractions of maritime life zones. For example, in the Amazon Basin, tropical dry forests have been displaced by tropical moist forests. In West Africa, tropical very dry forest changed to tropical thorn woodland, and tropical thorn woodland changed to desert scrub. On several Indonesian islands, under changing monsoon patterns, tropical moist forests expanded eastward, displacing subtropical wet forests.

3.3 | Future life zone changes

Life zone changes in our projections for the 21st century were much more pronounced than changes observed to date (Figures 2 and 3). Approximately 62 million km^2 (42.6%) of Earth's land surface were projected to change to a new life zone by 2070 under a business-as-usual carbon emissions scenario (RCP8.5)—more than double the area that changed during the 20th century (Figure 3c). This represents a life zone lapse rate of 0.57% per year, a 267% increase over the past century.

Under this scenario, 17 life zones (38%) are expected to contract by more than a third of their current size, while only 11 life zones (24%) are expected to expand by a similar amount (Figure 2b). Life zones associated with tropical wet forest, tropical rain forest, and cool temperate moist forest are projected to experience the largest percentage of area increases, while subpolar rain tundra, wet tundra, and moist tundra are projected to experience the largest percentage of area decreases (Figure 2). Boreal and polar latitudes are projected to experience substantial losses of area, though their vast extent makes these losses appear relatively small in percentage terms (Figure 3c).

Under a less severe emissions scenario (RCP4.5), approximately 41 million km^2 (28.4% of land) were projected to change to a new life zone by 2070, still more than 1.5 times the extent of 20th century life zone changes (Figures 2a and 3b). Compared to the high emissions scenario (RCP8.5), fewer life zone changes under RCP4.5 were projected in regions across Canada, Europe, northern Central Asia, northern and southern Africa, east Asia, and central Australia (Figure 3b).

FIGURE 2 Life zone area changes across historical (1901–1920), contemporary (1979–2013), and future (2061–2080) periods, where future calculations are based on RCP4.5 (a) versus RCP8.5 (b). Biotemperature classes are distinguished by black bounding boxes and labeled numerically, and life zones are colored by their historical classification, with colors given by legend in Figure 1
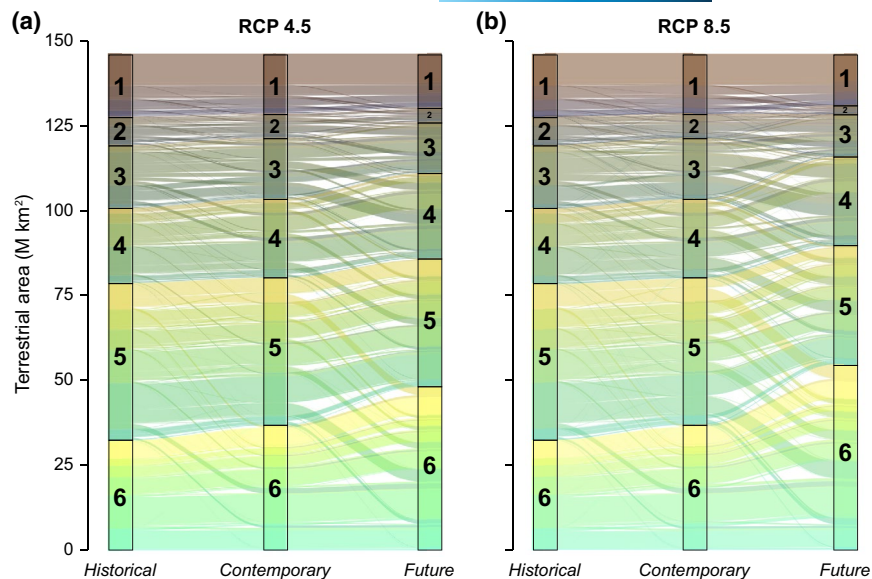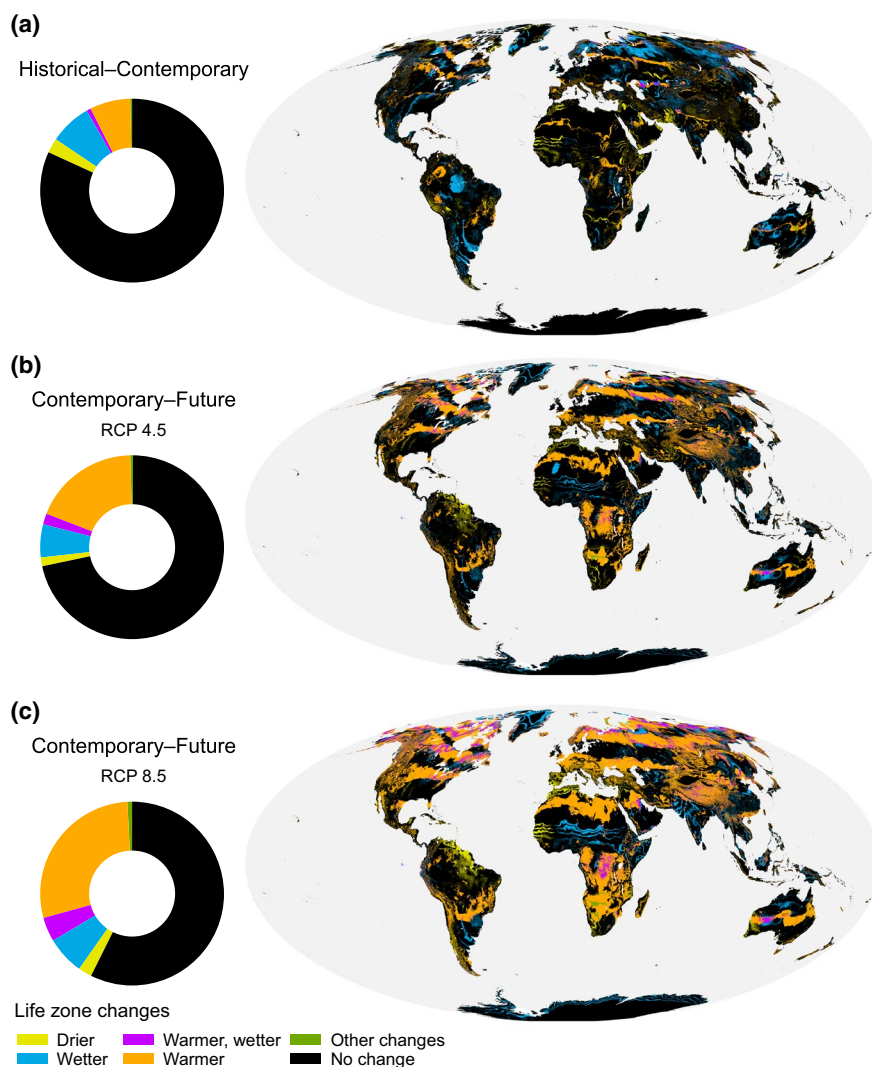

FIGURE 3 Changes in the distribution of life zones from (a) historical (1901–1920) to contemporary (1979–2013) periods, (b) contemporary to future (2061–2080) periods under RCP4.5, and (c) contemporary to future periods under RCP8.5. Inset donut plots show the proportions of each change type per change period

As with 20th-century patterns, life zones were projected to shift poleward and to higher elevations (Figures 1 and 3). Along the southern border of the Sahara, latitudinal bands of life zones change from desert to desert scrub, from desert scrub to thorn woodland, and from thorn woodland to very dry forest zones. Similarly, along elevational gradients in the Himalayas, life zones change from boreal rain

forests to cool temperate wet forests, and from cool temperate wet forests to warm temperate moist forests. Continental reductions in maritime influence also occur, notably with cool temperate steppe replaced by subtropical woodland in the southwestern United States.

Approximately 84 million km^2 (57.4% of land area) is projected to remain within the same life zone by 2070, even under the RCP8.5 emissions scenario (Figure 3c). The most extensive areas with stable life zones occur in midlatitude regions of the Amazon and Congo Basins, the Sahara Desert, Southeast Asia, and southern Australia.

3.4 | Life zone changes within biomes and ecoregions

Between the historical and contemporary periods, the biomes with the largest percentages of area changing life zones were Boreal Forests (36.8% of total biome area), Temperate Coniferous Forests (22.2%), and Tropical Coniferous Forests (20.1%; Figure 4a). In terms of absolute area, the least stable biomes were Deserts and Xeric Shrublands; Tropical Grasslands, Savannas, and Shrublands; and Tropical Moist Broadleaf Forests. Projections of changes between the contemporary period and 2070 under RCP8.5 were much more severe: 73.6% of Boreal Forests, 67.9% of Montane Grasslands and Shrublands, and 58.6% of Temperate Coniferous Forests (Figure 4c).

On average, 19.0% of the area of a given biome changed to a new life zone between historical and contemporary periods, compared with 43.3% projected between contemporary and future periods

(Figures 4c and 5). The greatest increases in percentage of area changed over time occurred in Montane Grasslands and Shrublands, Boreal Forests, Temperate Coniferous Forests, and Deserts and Xeric Shrublands (Figure 5b). As expected, within biomes, changes tended to be greater for colder life zones and less pronounced for warmer life zones. Tropical Coniferous Forests were the only biome to experience less loss between the contemporary to future periods than between the historical to contemporary periods (Figure S3; Figure 5c).

Between historical and contemporary periods, only 30 ecoregions (3.5%) had half or more of their total areas change to a new life zone (Figure 4d). The Red River Freshwater Swamp Forests of Vietnam, the Monte Alegre Várzea of Brazil, and the Indus Valley of Pakistan had the greatest proportional changes of life zones, each with over 75%. By 2070 under RCP8.5, seven ecoregions are projected to have a complete turnover of life zones, for example, the Serengeti Volcanic Grasslands of Tanzania, the Southeast Mixed Woodlands and Savannas of the United States, and the Tigris-Euphrates Alluvial Salt Marsh spanning the borders of Iraq and Iran. Under this scenario, a total of 281 ecoregions (33.2%) are projected to have half or more of their total area transition to a different life zone by 2070 (Figure 4f). This number is reduced to 111 ecoregions (13.1%) under the RCP4.5 emissions scenario (Figure 4e). The correlation between the magnitude of past and future life zone changes within biomes was high and positive (Pearson's $r = 0.7$), but there were both cases where projected mean magnitudes of change were similar to historical mean magnitudes of change (e.g., Tropical
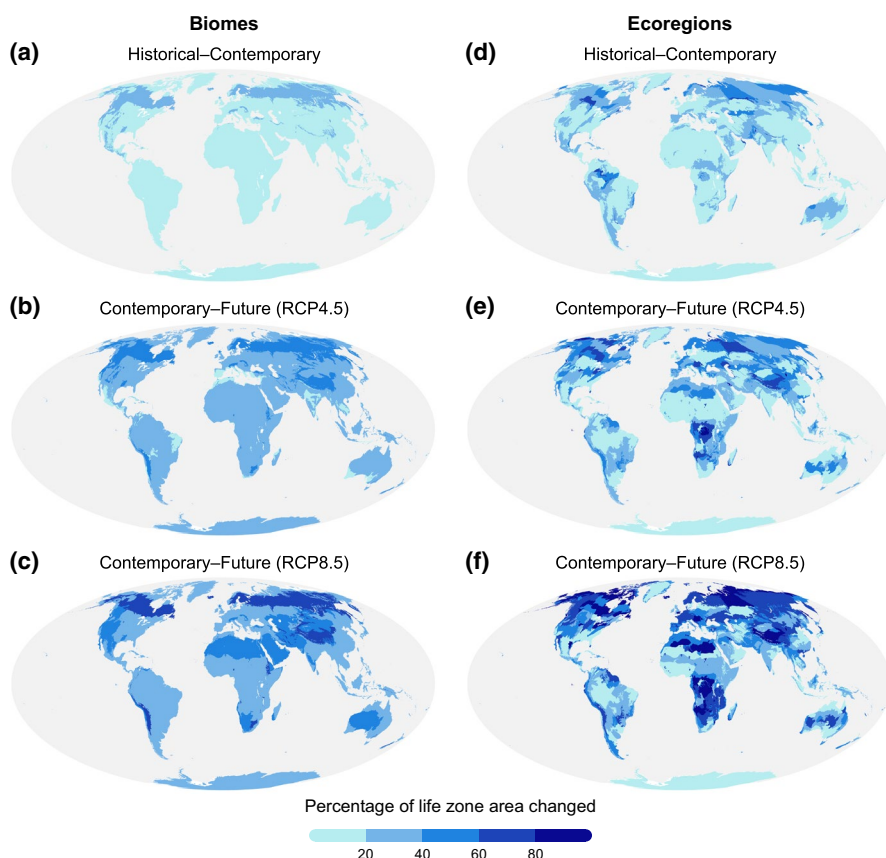

Biomes

(a) Historical–Contemporary

(b) Contemporary–Future (RCP4.5)

(c) Contemporary–Future (RCP8.5)

Ecoregions

(d) Historical–Contemporary

(e) Contemporary–Future (RCP4.5)

(f) Contemporary–Future (RCP8.5)

Percentage of life zone area changed

20 40 60 80

FIGURE 4 Global distribution of life zone changes within biomes (a–c) and ecoregions (d–f) as a percentage of biome/ecoregion area for historical (1901–1920) to contemporary (1979–2013) periods (top row), contemporary to future (2061–2080) periods under RCP4.5 (middle row), and contemporary to future periods under RCP8.5 (bottom row)
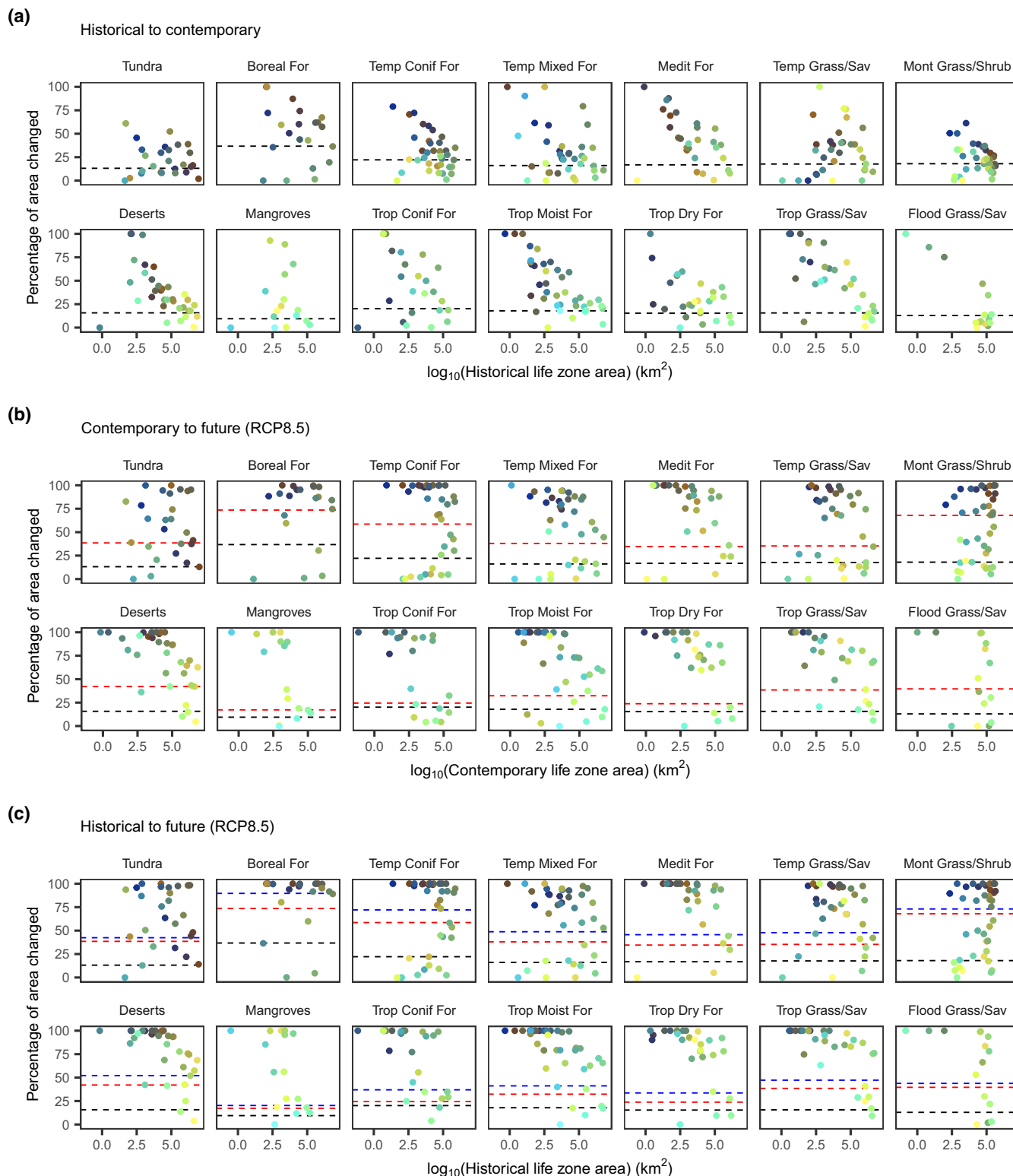
(a) Historical to contemporary

(b) Contemporary to future (RCP8.5)

(c) Historical to future (RCP8.5)

FIGURE 5 Life zone changes within biomes for (a) historical (1901–1920) to contemporary (1979–2013) periods, (b) contemporary to future (2061–2080) periods under RCP4.5, and (c) contemporary to future periods under RCP8.5. Each point represents a life zone (colored as in Figure 1) ordinated by life zone area of the baseline period considered and the percentage of life zone area that changed from one zone to another between the two periods in each panel. Facets represent biomes with abbreviated names (full names given in Table S2). Horizontal dashed black, red, and blue lines are mean percentages of area changed across life zones per biome for the historical to contemporary comparison, contemporary to future comparison, and historical to future comparison, respectively

Coniferous Forests had projected change only 1.2 times the extent of historical change) and where future magnitudes of change are projected to far exceed historical magnitudes of change (e.g., Montane Grasslands and Shrublands had projected change approximately 3.8 times the extent of historical change) (Figures 4c and 5b).

3.5 | Life zone changes and biodiversity, agriculture, and human population patterns

Among ecoregions, the percentage of life zone area change was weakly negatively correlated with mean threatened vertebrate richness (Pearson's $r = -0.12$; Figure 6a), the natural logarithm of mean vertebrate range size rarity ($r = -0.13$; Figure 6b), and the percentage of ecoregion cropland (Pearson's $r = -0.19$; Figure 6c). The GAM fits for these data indicated that the relationships were approximately linear. The percentage of life zone area change was also weakly negatively correlated with the natural logarithm of population density (Pearson's $r = -0.13$), though GAM fits indicated this relationship was weakly unimodal (Figure 6d). Density plots for all comparisons further showed no apparent relationships between biodiversity,
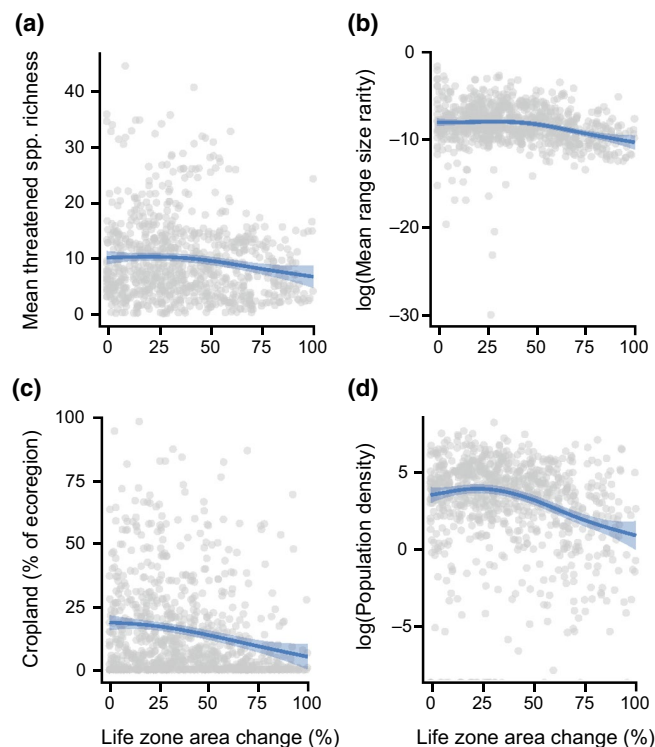

FIGURE 6 Relationships between life zone area change and (a) mean threatened vertebrate richness, (b) mean vertebrate range size rarity (on log scale), (c) the percentage of ecoregion under cropland, and (d) human population density (on log scale) among ecoregions (gray points, $n = 847$). Solid blue lines are model fits from generalized additive models using cubic regression splines and fitted with restricted maximum likelihood estimation; shaded blue areas reflect 95% confidence intervals

agriculture, or human population patterns and the percentage of life zone area changes within ecoregions (Figure S4).

3.6 | Uncertainty in future life zone classifications

Life zone classifications were fairly consistent among the five GCMs examined (Figure 7a; Figures S5 and S6). Approximately 99% and 98% of pixels were classified as the same life zone for at least four of the five GCMs considered for RCP4.5 and RCP8.5 scenarios, respectively (Figure 7a). There was slightly less agreement among GCMs in the RCP8.5 scenario, consistent with it having greater changes in climate parameters. Discrepancies among GCMs occurred in parts of the Amazon Basin, in latitudinal bands along the southern edge of the Sahara Desert, and in western South Asia and Australia (Figure 7a). Much of this variation reflects divergent precipitation projections among GCMs. Given that the GCMs were selected to minimize interdependence, the results validate that our method for deriving life zones is robust to the choice of GCM.

There were several large areas where similar life zone changes are projected under both RCP8.5 and RCP4.5. These were primarily located at northern latitudes (e.g., along a latitudinal band of northern Europe and in sporadic patches of Canada and across Russia), in the northern Amazon, in the horn of Africa, and in Western Australia (Figure 7b). Elsewhere, the larger areas of change in RCP8.5 often appeared as further poleward, elevational, and continental extensions of changes observed in RCP4.5. We identified divergent patterns in life zones changes between RCPs in northern Canada, the northern United States, in a latitudinal band of central Europe, across a large swath of Russia, in the northern Sahara, in southern Africa, and in sporadic patches of south Asia and central Australia (Figure 7b).

3.7 | Drivers of future life zone changes

Overall, future life zone changes are predominantly driven by warming temperatures (Figure 3c). Such changes are widely distributed across the northern hemisphere, along the Andes, in eastern and southern Africa, and along a latitudinal belt across northern and central Australia. Changes to cooler life zones were rare during the 20th century and absent from all future scenarios. Life zone changes arose from both increases in precipitation (e.g., in Greenland, along the Antarctic coast, in the Sahel, and in Punjab) and decreases in precipitation (e.g., in the Maghreb and the Guyana shield).

4 | DISCUSSION

Our analysis provides the first set of life zone maps from three distinct periods spanning 180 years using a consistent analytical framework at a global scale, yet with sufficient spatial resolution to guide local adaptation strategies. This has enabled a rigorous assessment

FIGURE 7 An assessment of life zone classification uncertainty, including the degree of life zone classification agreement (a) across five GCMs for RCP4.5 and RCP8.5 and (b) for a future (2061–2080) ensemble mean of five GCMs under RCP4.5 and RCP8.5. Inset donut plots in (a) show the proportions of classifications in agreement by the number of GCMs and in (b) show the proportions of life zone changes for different period comparisons
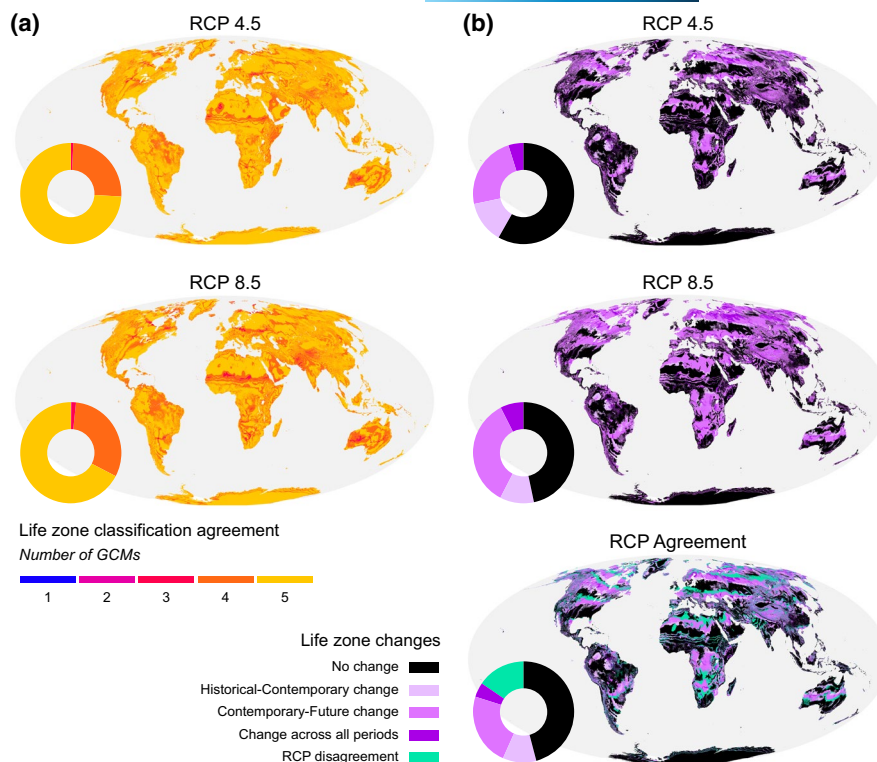
of both past and expected changes in life zone distributions and revealed that the pace of life zone change will nearly triple the annual rates experienced over the last century if emission rates are not dramatically reduced. Projected changes are unequally distributed across the globe, in patterns that depart from existing models of univariate climate change. Such changes are most extensive in boreal and subtropical zones and in regions with fewer croplands and lower population densities, though many densely populated areas that have not experienced such changes historically are also projected to experience substantial life zone changes. The lack of a strong relationship between the magnitude of projected changes and the number of threatened species and level of vertebrate endemism suggests that projected changes are likely to impact regions of low, moderate, and high threatened richness and endemism with relative uniformity. Altogether, our results suggest that adaptive conservation and sustainable development strategies will be substantially challenged in the coming decades, and our results help to pinpoint where such challenges may be most acute.

At the same time, our results also reveal vast landscapes where life zones have been stable and are projected to remain stable over the next 50 years, which may constitute climate refugia. Stable life zones disproportionately occur in remote areas with more extreme climates and few human settlements, including polar regions, the Sahara Desert, and the Amazon Basin. Nevertheless, stable life zones at the peripheries of life zone space are still projected to experience large increases in temperature and fluctuations in precipitation, which may stress the tolerances of some organisms and people living in these already climatically harsh environments. This is because the persistence of life zones is defined by mean climate parameters and does not exclude the possibility of significant shifts

in the frequency and severity of extreme events, such as recent fires across Australia (Dowdy et al., 2019; Ward et al., 2020b), or other changes to vegetation caused by human activities.

4.1 | Contrasting life zone and climate changes

The spatial distribution of life zone changes reported here reveals important differences compared to metrics aimed at capturing climate change, such as climate velocity (Burrows et al., 2011; Loarie et al., 2009), climatic dissimilarity (Belote et al., 2018), and niche exposure (Xu et al., 2020). Life zone delineations operate logarithmically, consistent with observed patterns of vegetation changes along climatic gradients (Holdridge, 1967), whereas climate change metrics typically operate linearly. Thus, small changes in climate parameters are more likely to result in life zone changes for zones at lower climate extremes (e.g., colder, drier, and less arid) than in zones at higher climate extremes. Consequently, whereas climate velocity and niche exposure metrics peak in regions with harsh climates, such as the Amazon Basin, the Sahara Desert, the Indian subcontinent, and northern Australia (Loarie et al., 2009; Xu et al., 2020), the degree of climate exposure is only projected to lead to sporadic changes in life zones in these regions (Figure 3). Thus, toward the upper bounds of climate parameter space, there is a larger decoupling of climate change and life zone changes that should be acknowledged in climate impact assessments.

Additional discrepancies between life zone and climate change metrics are due to thresholds that delineate transitions between discrete life zones as well as the influence of multiple climate variables on life zone distributions versus the singular influence in univariate

climate models, like thermal exposure (Xu et al., 2020). Because vegetation distributions are likely influenced by a range of climatic parameters (Kreft & Jetz, 2007), the use of multivariate climate parameters is necessary to enable more realistic expectations of the impacts of climate change on ecosystems.

4.2 | Consequences of life zone changes for ecosystems, ecoregions, and biomes

Life zones broadly represent landscape-scale ecosystem types (Holdridge, 1947), thus changes in life zones are indicative of potential ecosystem change. Yet it is important to recognize that ecosystem formations are driven by a suite of factors not accounted for in our models, and thus our results likely underestimate, to some degree, the amount of ecosystem change expected under climate change. For instance, our analysis provides details on the locations of suitable climate parameters to theoretically support life zones, but additional processes, such as wildfire dynamics, biotic interactions, pathogen distributions, and certain edaphic factors influence the finer scale distributions of ecosystems and their potential to either persist within changing climates or successfully track climatic factors across a landscape (Gonzalez et al., 2010). Such landscape-scale processes can have severe impacts on vegetation cover over broad extents. For example, rapid fire regime shifts in the Mediterranean Basin were driven by increases in fuel conditions and biomass connectivity following land abandonment and afforestation (Pausas & Fernández-Muñoz, 2012). Furthermore, abiotic stressors, such as drought, limited food availability and influenced mammalian grazing patterns to the point where they maintained altered vegetative states in African savannas (Sinclair et al., 2007).

Human activities can also radically alter ecosystem characteristics through degradative processes or through nutrient supplementation to either reduce or increase ecosystem adaptation potential, respectively (Vitousek et al., 1997). For example, pronounced livestock grazing in alpine grasslands limits tree recruitment and inhibits treeline advance at tropical cloud forest-grassland ecotones, even when changing temperatures would otherwise favor tropical forest establishment (Rehm & Feeley, 2015). Moreover, habitat modification can drive both downslope and upslope range shifts in ways that contradict or exacerbate expected species responses driven by climate change (Elsen et al., 2020b; Lenoir et al., 2010). The effects of humans on ecological systems are now so pervasive that few true pressure-free areas remain, which challenges both fine- and broad-scale projections of ecosystem change that do not explicitly consider sociocultural systems (Ellis, 2015). Future research should investigate how current patterns of anthropogenic pressure interact with projected life zone changes to reveal regions where these multiple threats align and amplify one another, as well as regions largely devoid of human pressure and with stable climates that may constitute "Anthropocene refugia" (Saxon, 2008).

Nevertheless, regions undergoing life zone changes are still indicative of vulnerability because they lack the fundamental, often limiting,

climatic factors necessary for proper function; thus our results are important in highlighting broad regions of overall concern. This is further elucidated by our investigation of life zone changes within biomes and ecoregions (Figures 4 and 5). Our results indicate that all biomes have experienced life zone transitions during the 20th century to some degree. Weighted by biome area, Boreal Forests, Temperate Coniferous Forests, and Tropical Coniferous Forests experienced the largest changes in life zone distributions during this period. Ecoregions within these biomes have seen similar magnitudes of change.

A previous assessment based on climate change exposure metrics alone concluded that tundra, boreal forests, mountainous regions, Mediterranean ecosystems, and tropical rainforests are the most vulnerable ecosystems to climate change (Bernstein et al., 2008). Another assessment, which directly accounted for biome sensitivity and resilience in addition to exposure, found that Deserts and Xeric Shrublands is the most vulnerable biome (Li et al., 2018). Consistent with these findings, we identified Boreal Forests, Montane Grasslands and Shrublands, Temperate Coniferous Forests, and Deserts and Xeric Shrublands as the top four biomes projected to experience the largest life zone changes. However, contrary to both these previous assessments, our findings indicate that the Temperate Coniferous Forests biome may also be particularly vulnerable due to large projected shifts in life zones, especially in the cooler portions of parameter space.

Our ecoregion-level analysis revealed important nuances not illustrated within the biome-level analysis. Most importantly, our analysis indicated high variability among ecoregions in historical life zone changes, which are projected to be exacerbated over the next 50 years. Our results are similar to previous projections of ecoregion climate stability based on multivariate climate similarity metrics, including several temperature and precipitation-related parameters at a much coarser (2.5 arc-min) spatial resolution (Watson et al., 2013), but differ from assessments that analyzed thermal exposure within ecoregions relative to a baseline degree of temperature variability experienced (Beaumont et al., 2011). Watson et al. (2013) reported ecoregions with relatively low climate stability at high latitudes and altitudes and higher climate stability at low latitudes across a wide range of altitudes. Our results largely mirror this finding, as ecoregions found throughout the Amazon Basin, western Africa, and northern Australia had only a small percentage of area changing to a new life zone by 2070. Notable differences include ecoregions in southern Patagonia, which are projected to experience large shifts in life zones in our analysis, but have relatively stable climates in Watson et al. (2013). This again may be explained by small changes in climate parameters leading to larger life zone changes in colder regions due to the logarithmic scale of life zone parameter space. Other observed differences are likely due to the differences in spatial resolutions of datasets used (30 arc-sec vs. 2.5 arc-min). Still, the overall high concordance of our results with this previous assessment, combined with new knowledge of how life zones have already changed within ecoregions during the 20th century, underscores concerns about future adaptation potential within ecoregions and the limitations of considering ecoregions to be static spatial units with which to measure progress toward conservation targets (Smith et al., 2018).

Our modeling results are also consistent with documented changes in vegetation patterns at landscape scales. For example, the life zone shifts we observed in West Africa are reflected in empirical observations of shifts in regional woody vegetation patterns (Niang et al., 2014). Furthermore, historical life zone changes along the elevational gradient of Chimborazo in the Ecuadorian Andes closely reflect empirically documented upslope vegetation shifts (Morueta-Holme et al., 2015). At the same time, our models highlight projected changes in vegetation that deviate from recent changes and long-standing patterns. For example, drought-induced shifts in the Ponderosa pine-Piñon juniper ecotone in New Mexico, USA since the 1950s (Allen & Breshears, 1998) are not captured by our models, though regions just south do show a transition from cool temperate steppe to subtropical thorn woodland over the 20th century. This could be because the ecological processes leading to this change were not incorporated in our models, or because they operate at finer spatial scales than our models were able to capture. Additionally, along the northern border of the Sahara, our models indicate that desert zones will expand nearly to the Mediterranean coast, massively extending the footprint of a desert ecosystem that was established approximately 2700 years ago (Kröpelin et al., 2008).

4.3 | Consequences of life zone changes for livelihoods and people

Unstable life zones raise concerns for people due to the disruption of environmental conditions that currently support human livelihoods (Pecl et al., 2017). For example, drying of life zones in the Aegean and Mediterranean regions has already marginalized agroecosystems (Tatli & Dalfes, 2015). Future changes to extensively warmer (e.g., European Mediterranean region) and drier (e.g., African Mediterranean region) life zones may exacerbate these impacts. Changes in precipitation and evapotranspiration patterns in the Yellow River Basin in China since the 1960s have also already led to changes in runoff and streamflow dynamics that have altered water availability for agriculture in downstream communities (Cuo et al., 2013). In Africa, desert encroachment has already been observed, and warming temperatures are expected to reduce yields of most major cereal crops in much of sub-Saharan Africa (Niang et al., 2014). Our models project life zones in sub-Saharan Africa will change to warmer and wetter life zones, which will have direct impacts on growing season length and may shift the distribution of crop production, which is heavily influenced by levels of rainfall and aridity (Muimba-Kankolongo, 2018). Furthermore, the distribution of important timber species in Europe is expected to shift under climate change, resulting in a significant reduction in land values (Hanewinkel et al., 2013).

Consistent with our results, other recent analyses predict drylands will expand globally due to increasing aridity and temperatures. Land degradation and desertification will require stricter water resource management and more soil and vegetation restoration (Huang et al., 2015). This will be especially important in regions like the Dry Chaco of Paraguay and northwestern Argentina, where future life zone shifts from subtropical dry forest to tropical very dry forest will likely further reduce the availability of water needed to support the recent rapid expansion and intensification of agriculture (Baumann et al., 2017). Adaptation measures, including more conservative irrigation and water use policies, and altered timing and composition of crop plantings, will be increasingly needed to attenuate disruptions to food supply chains (Iglesias & Garrote, 2015; Lehmann et al., 2013).

Even in climates where moisture is not currently a limiting factor, life zone changes will disrupt resource availability and productivity. Areas that are currently highly suitable for croplands are expected to decline in the tropics, leading to projected declines in overall agricultural productivity (Zabel et al., 2014). The projected expansion of life zones suitable for croplands across many northern latitude regions may undermine the health of forested lands and protected areas without affecting other limits to cropping, such as infertile soils and short day length (Zabel et al., 2014). Failure to match transitions in life zones with transitions in land use will have unintended social and environmental impacts, such as land use conflicts, loss of environmental services, and accelerated greenhouse gas emissions (Tilman et al., 2011). Life zone changes could even impact carbon cycling and the global carbon budget. For example, projected changes across large portions of Southeast Asia show life zones associated with more carbon-rich montane forests replaced with those associated with lowland forests that store relatively lower amounts of carbon in the region (Feng et al., 2021).

While the most extensive life zone changes are projected to occur in regions characterized by less cropland cover, this relationship is fairly weak and there are notable exceptions, including the Southern Great Lakes Forests ecoregion in the United States and the Pannonian Mixed Forests ecoregion of eastern Europe, where >50% of each ecoregion is cropland and where 87%–93% of their total areas are projected to change to a different life zone. These examples highlight that a number of landscapes with communities that are highly dependent on agriculture will likely face substantial impacts owing to life zone changes impacting the climatic suitability for current crop types and the frequency, timing, and duration of cropping.

Impacts from life zone changes will also affect both remote and densely populated places. Life zones in some regions of low population density, like the Sahara Desert and Amazon Basin, are projected to remain relatively stable, whereas others, like the Boreal Forests of North America, are projected to experience extensive changes. Similarly, some heavily populated regions, such as the Southeast United States Mixed Woodlands and Savannas, are projected to experience life zone changes in >90% of the ecoregion, while others, like the Central African Mangroves in coastal West Africa, are projected to remain relatively stable.

4.4 | Consequences of life zone changes for biodiversity

Life zone changes will likely redefine distributional limits of species and disrupt ecological functions (Pecl et al., 2017; Scheffers et al., 2016). For example, the contractions of high elevation life zones in the Himalayas will likely reduce suitable habitat for endemic biodiversity, while also diminishing permafrost and increasing the volatility of hydrological regimes (Xu et al., 2009). Established conservation mechanisms, currently operating within life zones incorrectly assumed to be stable, must refocus on programs that enhance adaptive capacity (Reside et al., 2018; Scheffers et al., 2016). Habitat management actions that enable ecosystem shifts, increase connectivity to facilitate species movement, and protect localized microclimates to buffer species against climate extremes will be especially important in areas expected to experience the most rapid and extensive life zone changes (Heller & Zavaleta, 2009; Ward et al., 2020a). As a consequence, efforts to retain ecosystem integrity will be increasingly important as an adaptation strategy to build climate resilience and minimize potential species extinctions associated with life zone changes (Martin & Watson, 2016).

Today, regions with a long history of climate stability are associated with high species richness, species endemism, and lower extinction rates (Brown et al., 2020). Looking forward, our results suggest that regions of both low and high vertebrate species richness and endemism will face substantial life zone changes. For example, our results point to a nearly 50% turnover in life zone area for some of the most species-rich and highly endemic ecoregions, such as the Borneo Montane Rain Forests ecoregion of Indonesia and the South Western Ghats Montane Rain Forests ecoregion of India by 2070. Such rapid changes could potentially challenge species' adaptive capacities. Consequently, places that will experience the least climate change in the near future—and places where life zones will persist unchanged—represent those with the highest potential for Anthropocene refugia (Monsarrat et al., 2019; Saxon, 2008). Provided that local extinction does not occur there due to non-climate factors, stable life zones provide the places where biodiversity is most likely to persist, adapt (Morelli et al., 2016; Watson et al., 2013), and even speciate (Brown et al., 2020).

5 | SUMMARY

New evidence shows the highly dynamic nature of life zones, the boundaries of which have already changed substantially over the past century. Importantly, the projected rate of future life zone change is much faster than the past, including in most ecoregions and within all biomes on Earth. Our high-resolution data provide the basis for temporal and spatial discrimination in the allocation of climate-adaptive conservation and sustainable development strategies. Policies and practices that are mismatched with life zone changes are likely to misallocate their limited resources and fail to meet biodiversity conservation goals and SDGs, especially in regions where the pace of change is greatest and the climatological thresholds for failure are already near.

DATA AVAILABILITY STATEMENT

Data used in this manuscript are freely available at the following websites:

Climate data: CHELSA climate data: https://chelsa-climate.org/. Potential evapotranspiration data: CGIAR PET data: https://cgiarcsi.community/data/global-aridity-and-pet-database/. Terrestrial ecoregion data: Biome/ecoregion data: https://ecoregions2017.appspot.com/. Richness and range size rarity data: https://www.iucnredlist.org/resources/other-spatial-downloads/. Original life zone data produced in this manuscript for historical, contemporary, and future periods are openly available in Dryad at https://doi.org/10.5061/dryad.41ns1rnff.

ORCID

Paul R. Elsen https://orcid.org/0000-0002-9953-7961
Earl C. Saxon https://orcid.org/0000-0002-7646-1298
B. Alexander Simmons https://orcid.org/0000-0002-1918-3463
Michelle Ward https://orcid.org/0000-0002-0658-855X
Brooke A. Williams https://orcid.org/0000-0002-0692-7507
Hedley S. Grantham https://orcid.org/0000-0002-8933-807X
Salit Kark https://orcid.org/0000-0002-7183-3988
Noam Levin https://orcid.org/0000-0002-9434-7501
Katharina-Victoria Perez-Hammerle https://orcid.org/0000-0002-2434-5594
April E. Reside https://orcid.org/0000-0002-0760-9527
James E. M. Watson https://orcid.org/0000-0003-4942-1984

REFERENCES

Adger, W. N., Barnett, J., Brown, K., Marshall, N., & O'Brien, K. (2013). Cultural dimensions of climate change impacts and adaptation. *Nature Climate Change*, *3*, 112–117. https://doi.org/10.1038/nclimate1666

Allen, C. D., & Breshears, D. D. (1998). Drought-induced shift of a forest-woodland ecotone: Rapid landscape response to climate variation.

Proceedings of the National Academy of Sciences USA, *95*, 14839–14842. https://doi.org/10.1073/pnas.95.25.14839

Batllori, E., Parisien, M.-A., Parks, S. A., Moritz, M. A., & Miller, C. (2017). Potential relocation of climatic environments suggests high rates of climate displacement within the North American protection network. *Global Change Biology*, *23*, 3219–3230. https://doi.org/10.1111/gcb.13663

Baumann, M., Gasparri, I., Piquer-Rodríguez, M., Pizarro, G. G., Griffiths, P., Hostert, P., & Kuemmerle, T. (2017). Carbon emissions from agricultural expansion and intensification in the Chaco. *Global Change Biology*, *23*, 1902–1916. https://doi.org/10.1111/gcb.13521

Beaumont, L. J., Pitman, A., Perkins, S., Zimmermann, N. E., Yoccoz, N. G., & Thuiller, W. (2011). Impacts of climate change on the world's most exceptional ecoregions. *Proceedings of the National Academy of Sciences USA*, *108*, 2306–2311. https://doi.org/10.1073/pnas.1007217108

Beck, H. E., Zimmermann, N. E., McVicar, T. R., Vergopolan, N., Berg, A., & Wood, E. F. (2018). Present and future Köppen-Geiger climate classification maps at 1-km resolution. *Scientific Data*, *5*, 1–12. https://doi.org/10.1038/sdata.2018.214

Bellard, C., Bertelsmeier, C., Leadley, P., Thuiller, W., & Courchamp, F. (2012). Impacts of climate change on the future of biodiversity. *Ecology Letters*, *15*, 365–377. https://doi.org/10.1111/j.1461-0248.2011.01736.x

Belote, R. T., Carroll, C., Martinuzzi, S. X. N., Michalak, J., Williams, J. W., Williamson, M. A., & Aplet, G. H. (2018). Assessing agreement among alternative climate change projections to inform conservation recommendations in the contiguous United States. *Scientific Reports*, *8*, 9441. https://doi.org/10.1038/s41598-018-27721-6

Bergengren, J. C., Waliser, D. E., & Yun, Y. L. (2011). Ecological sensitivity: a biospheric view of climate change. *Climatic Change*, *107*, 433–457. https://doi.org/10.1007/s10584-011-0065-1

Bernstein, L., Bosch, P., Canziani, O., Chen, Z., Christ, R., & Riahi, K. (2008). *IPCC, 2007: Climate Change 2007: Synthesis Report*. IPCC.

Bond, W. J. (2005). Large parts of the world are brown or black: A different view on the 'Green World' hypothesis. *Journal of Vegetation Science*, *16*, 261–266. https://doi.org/10.1658/1100-9233(2005)016%5B0261:LPOTWA%5D2.0.CO;2

Box, E. O. (1996). Plant functional types and climate at the global scale. *Journal of Vegetation Science*, *7*, 309–320. https://doi.org/10.2307/3236274

Brown, S. C., Wigley, T. M. L., Otto-Bliesner, B. L., Rahbek, C., & Fordham, D. A. (2020). Persistent Quaternary climate refugia are hospices for biodiversity in the Anthropocene. *Nature Climate Change*, *10*, 244–248. https://doi.org/10.1038/s41558-019-0682-7

Burrows, M. T., Schoeman, D. S., Buckley, L. B., Moore, P., Poloczanska, E. S., Brander, K. M., Brown, C., Bruno, J. F., Duarte, C. M., Halpern, B. S., Holding, J., Kappel, C. V., Kiessling, W., O'Connor, M. I., Pandolfi, J. M., Parmesan, C., Schwing, F. B., Sydeman, W. J., & Richardson, A. J. (2011). The pace of shifting climate in marine and terrestrial ecosystems. *Science*, *334*, 652–655. https://doi.org/10.1126/science.1210288

Carroll, M. L., Townshend, J. R., DiMiceli, C. M., Noojipady, P., & Sohlberg, R. A. (2009). A new global raster water mask at 250 m resolution. *International Journal of Digital Earth*, *2*, 291–308. https://doi.org/10.1080/17538940902951401

Center for International Earth Science Information Network – CIESIN – Columbia University. (2018). Gridded Population of the World, Version 4 (GPWv4): Population Density, Revision 11 (NASA Socioeconomic Data and Applications Center (SEDAC). Accessed June 2021).

Chen, J., Chen, J., Liao, A., Cao, X., Chen, L., Chen, X., He, C., Han, G., Peng, S., Lu, M., Zhang, W., Tong, X., & Mills, J. (2015). Global land cover mapping at 30m resolution: A POK-based operational approach. *ISPRS Journal of Photogrammetry and Remote Sensing*, *103*, 7–27. https://doi.org/10.1016/j.isprsjprs.2014.09.002

Convention on Biodiversity (CBD). (2011). *COP 10 Decision X/2: Strategic Plan for Biodiversity 2011–2020*.

Cuo, L., Zhang, Y., Gao, Y., Hao, Z., & Cairang, L. (2013). The impacts of climate change and land cover/use transition on the hydrology in the upper Yellow River Basin, China. *Journal of Hydrology*, *502*, 37–52. https://doi.org/10.1016/j.jhydrol.2013.08.003

Daru, B. H., Farooq, H., Antonelli, A., & Faurby, S. (2020). Endemism patterns are scale dependent. *Nature Communications*, *11*, 2115. https://doi.org/10.1038/s41467-020-15921-6

Dee, D. P., Uppala, S. M., Simmons, A. J., Berrisford, P., Poli, P., Kobayashi, S., Andrae, U., Balmaseda, M. A., Balsamo, G., Bauer, P., Bechtold, P., Beljaars, A. C. M., van de Berg, L., Bidlot, J., Bormann, N., Delsol, C., Dragani, R., Fuentes, M., Geer, A. J., … Vitart, F. (2011). The ERA-Interim reanalysis: configuration and performance of the data assimilation system. *Quarterly Journal of the Royal Meteorological Society*, *137*, 553–597. https://doi.org/10.1002/qj.828

Dinerstein, E., Olson, D., Joshi, A., Vynne, C., Burgess, N. D., Wikramanayake, E., Hahn, N., Palminteri, S., Hedao, P., Noss, R., Hansen, M., Locke, H., Ellis, E. C., Jones, B., Barber, C. V., Hayes, R., Kormos, C., Martin, V., Crist, E., … Saleem, M. (2017). An ecoregion-based approach to protecting half the terrestrial realm. *BioScience*, *67*, 534–545. https://doi.org/10.1093/biosci/bix014

Dowdy, A. J., Ye, H., Pepler, A., Thatcher, M., Osbrough, S. L., Evans, J. P., Di Virgilio, G., & McCarthy, N. (2019). Future changes in extreme weather and pyroconvection risk factors for Australian wildfires. *Scientific Reports*, *9*, 10073. https://doi.org/10.1038/s41598-019-46362-x

Droogers, P., & Allen, R. G. (2002). Estimating reference evapotranspiration under inaccurate data conditions. *Irrigation and Drainage Systems*, *16*, 33–45.

Ellis, E. C. (2015). Ecology in an anthropogenic biosphere. *Ecological Monographs*, *85*, 287–331. https://doi.org/10.1890/14-2274.1

Elsen, P. R., Monahan, W. B., Dougherty, E. R., & Merenlender, A. M. (2020a). Keeping pace with climate change in global terrestrial protected areas. *Science Advances*, *11*, eaay0814. https://doi.org/10.1126/sciadv.aay0814

Elsen, P. R., Monahan, W. B., & Merenlender, A. M. (2018). Global patterns of protection of elevational gradients in mountain ranges. *Proceedings of the National Academy of Sciences USA*, *115*, 6004–6009. https://doi.org/10.1073/pnas.1720141115

Elsen, P. R., Monahan, W. B., & Merenlender, A. M. (2020b). Topography and human pressure in mountain ranges alter expected species responses to climate change. *Nature Communications*, *11*, 1974. https://doi.org/10.1038/s41467-020-15881-x

Elsen, P. R., Saxon, E. C., Simmons, B. A., Ward, M., Williams, B. A., Grantham, H. S., Kark, S., Levin, N., Perez-Hammerle, K.-V., Reside, A. E., & Watson, J. E. M. (2021). Historical (1901–1920), contemporary (1979–2013), and future (2061–2080) terrestrial life zones. Dryad, https://doi.org/10.5061/dryad.41ns1rnff

Feng, Y., Ziegler, A. D., Elsen, P. R., Liu, Y., He, X., Spracklen, D. V., Holden, J., Jiang, X., Zheng, C., & Zeng, Z. (2021). Upward expansion and acceleration of forest clearance in the mountains of Southeast Asia. *Nature Sustainability*, *4*, 829–899. https://doi.org/10.1038/s41893-021-00738-y

Gonzalez, P., Neilson, R. P., Lenihan, J. M., & Drapek, R. J. (2010). Global patterns in the vulnerability of ecosystems to vegetation shifts due to climate change. *Global Ecology and Biogeography*, *19*, 755–768. https://doi.org/10.1111/j.1466-8238.2010.00558.x

Gorelick, N., Hancher, M., Dixon, M., Ilyushchenko, S., Thau, D., & Moore, R. (2017). Google Earth Engine: Planetary-scale geospatial analysis for everyone. *Remote Sensing of Environment*, *202*, 18–27. https://doi.org/10.1016/j.rse.2017.06.031

Guerin, G. R., & Lowe, A. J. (2015). 'Sum of inverse range-sizes' (SIR), a biodiversity metric with many names and interpretations. *Biodiversity and Conservation*, *24*, 2877–2882.

Guerin, G. R., Ruokolainen, L., & Lowe, A. J. (2015). A georeferenced implementation of weighted endemism. *Methods in Ecology and Evolution, 6*, 845–852. https://doi.org/10.1111/2041-210X.12361

Hanewinkel, M., Cullmann, D. A., Schelhaas, M.-J., Nabuurs, G.-J., & Zimmermann, N. E. (2013). Climate change may cause severe loss in the economic value of European forest land. *Nature Climate Change, 3*, 203–207. https://doi.org/10.1038/nclimate1687

Hanson, J. O., Rhodes, J. R., Butchart, S. H. M., Buchanan, G. M., Rondinini, C., Ficetola, G. F., & Fuller, R. A. (2020). Global conservation of species' niches. *Nature, 580*, 232–234. https://doi.org/10.1038/s41586-020-2138-7

Harris, I., Osborn, T. J., Jones, P., & Lister, D. (2020). Version 4 of the CRU TS monthly high-resolution gridded multivariate climate dataset. *Scientific Data, 7*, 109. https://doi.org/10.1038/s41597-020-0453-3

Hayhoe, K., Edmonds, J., Kopp, R. E., LeGrande, A. N., Sanderson, B. M., Wehner, M. F., & Wuebbles, D. J. (2017). Climate models, scenarios, and projections. In D. J. Wuebbles, D. W. Fahey, K. A. Hibbard, D. J. Dokken, B. C. Stewart, & T. K. Maycock (Eds.), *Climate Science Special Report: Fourth National Climate Assessment* (vol. I, 28 p.). U.S. Global Change Research Program.

Heller, N. E., & Zavaleta, E. S. (2009). Biodiversity management in the face of climate change: A review of 22 years of recommendations. *Biological Conservation, 142*, 14–32. https://doi.org/10.1016/j.biocon.2008.10.006.

Hirota, M., Holmgren, M., Van Nes, E. H., & Scheffer, M. (2011). Global resilience of tropical forest and savanna to critical transitions. *Science, 334*, 232–235. https://doi.org/10.1126/science.1210657

Holdridge, L. R. (1947). Determination of world plant formations from simple climatic data. *Science, 105*, 367–368. https://doi.org/10.1126/science.105.2727.367

Holdridge, L. R. (1967). *Life zone ecology.* Tropical Science Center.

Huang, J., Yu, H., Guan, X., Wang, G., & Guo, R. (2015). Accelerated dryland expansion under climate change. *Nature Climate Change, 6*, 166–171. https://doi.org/10.1038/nclimate2837

Iglesias, A., & Garrote, L. (2015). Adaptation strategies for agricultural water management under climate change in Europe. *Agricultural Water Management, 155*, 113–124. https://doi.org/10.1016/j.agwat.2015.03.014

IUCN (2021). The IUCN Red List of Threatened Species, version 3, May 2017. Accessed June 11, 2021. https://www.iucnredlist.org/resources/other-spatial-downloads

Karger, D. N., Conrad, O., Böhner, J., Kawohl, T., Kreft, H., Soria-Auza, R. W., Zimmermann, N. E., Linder, H. P., & Kessler, M. (2017). Data Descriptor: Climatologies at high resolution for the earth's land surface areas. *Scientific Data, 4*, 170122. https://doi.org/10.1038/sdata.2017.122

Keith, D. A., J. R. Ferrer-Paris, E. Nicholson, & R. T. Kingsford (Eds.) (2020). *The IUCN Global Ecosystem Typology 2.0: Descriptive profiles for biomes and ecosystem functional groups.* IUCN.

Kier, G., Kreft, H., Lee, T. M., Jetz, W., Ibisch, P. L., Nowicki, C., Mutke, J., & Barthlott, W. (2009). A global assessment of endemism and species richness across island and mainland regions. *Proceedings of the National Academy of Sciences USA, 106*, 9322–9327. https://doi.org/10.1073/pnas.0810306106

Kreft, H., & Jetz, W. (2007). Global patterns and determinants of vascular plant diversity. *Proceedings of the National Academy of Sciences USA, 104*, 5925–5930. https://doi.org/10.1073/pnas.0608361104

Kröpelin, S., Verschuren, D., Lézine, A.-M., Eggermont, H., Cocquyt, C., Francus, P., Cazet, J.-P., Fagot, M., Rumes, B., Russell, J. M., Darius, F., Conley, D. J., Schuster, M., von Suchodoletz, H., & Engstrom, D. R. (2008). Climate-driven ecosystem succession in the Sahara: The past 6000 years. *Science, 320*, 765–768. https://doi.org/10.1126/science.1154913

Laffan, S. W., & Crisp, M. D. (2003). Assessing endemism at multiple spatial scales, with an example from the Australian vascular flora. *Journal of Biogeography, 30*, 511–520. https://doi.org/10.1046/j.1365-2699.2003.00875.x

Latham, J., Cumani, R., Rosati, I., & Bloise, M. (2014). *Global land cover share (GLC-SHARE) database beta-release version 1.0-2014.* . Food and Agriculture Organization.

Lawler, J. J., Shafer, S. L., White, D., Kareiva, P., Maurer, E. P., Blaustein, A. R., & Bartlein, P. J. (2009). Projected climate-induced faunal change in the Western Hemisphere. *Ecology, 90*, 588–597. https://doi.org/10.1890/08-0823.1

Lehmann, N., Finger, R., Klein, T., Calanca, P., & Walter, A. (2013). Adapting crop management practices to climate change: Modeling optimal solutions at the field scale. *Agricultural Systems, 117*, 55–65. https://doi.org/10.1016/j.agsy.2012.12.011

Lenoir, J., Gégout, J.-C., Guisan, A., Vittoz, P., Wohlgemuth, T., Zimmerman, N. E., Dullinger, S., Pauli, H., Willner, W., & Svenning, J.-C. (2010). Going against the flow: potential mechanisms for unexpected downslope range shifts in a warming climate. *Ecography, 33*, 295–303. https://doi.org/10.1111/j.1600-0587.2010.06279.x

Li, D., Wu, S., Liu, L., Zhang, Y., & Li, S. (2018). Vulnerability of the global terrestrial ecosystems to climate change. *Global Change Biology, 24*, 4095–4106. https://doi.org/10.1111/gcb.14327.

Loarie, S. R., Duffy, P. B., Hamilton, H., Asner, G. P., Field, C. B., & Ackerly, D. D. (2009). The velocity of climate change. *Nature, 462*, 1052–1055. https://doi.org/10.1038/nature08649.

Lugo, A. E., Brown, S. L., Dodson, R., Smith, T. S., & Shugart, H. H. (1999). The Holdridge life zones of the conterminous United States in relation to ecosystem mapping. *Journal of Biogeography, 26*, 1025–1038. https://doi.org/10.1046/j.1365-2699.1999.00329.x

Martin, T. G., & Watson, J. E. M. (2016). Intact ecosystems provide best defence against climate change. *Nature Climate Change, 6*, 122–124. https://doi.org/10.1038/nclimate2918

Maxwell, S. L., Cazalis, V., Dudley, N., Hoffmann, M., Rodrigues, A. S. L., Stolton, S., Visconti, P., Woodley, S., Kingston, N., Lewis, E., Maron, M., Strassburg, B. B. N., Wenger, A., Jonas, H. D., Venter, O., & Watson, J. E. M. (2020). Area-based conservation in the twenty-first century. *Nature, 586*, 217–227. https://doi.org/10.1038/s41586-020-2773-z

Miller-Rushing, A. J., Lloyd-Evans, T. L., Primack, R. B., & Satzinger, P. (2008). Bird migration times, climate change, and changing population sizes. *Global Change Biology, 14*, 1959–1972. https://doi.org/10.1111/j.1365-2486.2008.01619.x.

Monsarrat, S., Jarvie, S., & Svenning, J.-C. (2019). Anthropocene refugia: integrating history and predictive modelling to assess the space available for biodiversity in a human-dominated world. *Philosophical Transactions of the Royal Society B: Biological Sciences, 374*, 20190219–20190310. https://doi.org/10.1098/rstb.2019.0219

Morelli, T. L., Daly, C., Dobrowski, S. Z., Dulen, D. M., Ebersole, J. L., Jackson, S. T., Lundquist, J. D., Millar, C. I., Maher, S. P., Monahan, W. B., Nydick, K. R., Redmond, K. T., Sawyer, S. C., Stock, S., & Beissinger, S. R. (2016). Managing Climate Change Refugia for Climate Adaptation. *PLoS One, 11*, e0159909. https://doi.org/10.1371/journal.pone.0159909

Morueta-Holme, N., Engemann, K., Sandoval-Acuña, P., Jonas, J. D., Segnitz, M., & Svenning, J.-C. (2015). Strong upslope shifts in Chimborazo's vegetation over two centuries since Humboldt. *Proceedings of the National Academy of Sciences USA, 112*, 12741–12745. https://doi.org/10.1073/pnas.1509938112

Muimba-Kankolongo, A. (2018). *Food Crop Production by Smallholder Farmers in Southern Africa: Challenges and Opportunities for Improvement – Chapter 2: Climates and Agroecologies.* Academic Press.

Neilson, R. P., Pitelka, L. F., Solomon, A. M., Nathan, R., Midgley, G. F., Fragoso, J. M. V., Lischke, H., & Thompson, K. (2005). Forecasting regional to global plant migration in response to climate change.

BioScience, *55*, 749–759. https://doi.org/10.1641/0006-3568(2005) 055%5B0749:FRTGPM%5D2.0.CO;2

Niang, I., Ruppel, O. C., Abdrabo, M. A., & Essel, A. (2014) *Climate Change 2014: Impacts, Adaptation, and Vulnerability. Part B: Regional Aspects. Contribution of Working Group II to the Fifth Assessment Report of the Intergovernmental Panel on Climate Change, chap. Africa.* Cambridge University Press, Cambridge, United Kingdom and New York, NY, 67 p.

Nolan, C., Overpeck, J. T., Allen, J. R. M., Anderson, P. M., Betancourt, J. L., Binney, H. A., Brewer, S., Bush, M. B., Chase, B. M., Cheddadi, R., Djamali, M., Dodson, J., Edwards, M. E., Gosling, W. D., Haberle, S., Hotchkiss, S. C., Huntley, B., Ivory, S. J., Kershaw, A. P., ... Jackson, S. T. (2018). Past and future global transformation of terrestrial ecosystems under climate change. *Science*, *361*, 920–923. https://doi.org/10.1126/science.aan5360

Olson, D. M., Dinerstein, E., Wikramanayake, E. D. et al (2001). Terrestrial ecoregions of the worlds: A new map of life on Earth. *BioScience*, *51*, 933–938.

Pan, Y., Li, X., Gong, P., He, C., Shi, P., & Pu, R. (2010). An integrative classification of vegetation in China based on NOAA AVHRR and vegetation-climate indices of the Holdridge life zone. *International Journal of Remote Sensing*, *24*, 1009–1027. https://doi.org/10.1080/01431160110115816

Pausas, J. G., & Fernández-Muñoz, S. (2012). Fire regime changes in the Western Mediterranean Basin: from fuel-limited to drought-driven fire regime. *Climatic Change*, *110*, 215–226. https://doi.org/10.1007/s10584-011-0060-6

Pecl, G. T., Araújo, M. B., Bell, J. D., Blanchard, J., Bonebrake, T. C., Chen, I.-C., Clark, T. D., Colwell, R. K., Danielsen, F., Evengård, B., Falconi, L., Ferrier, S., Frusher, S., Garcia, R. A., Griffis, R. B., Hobday, A. J., Janion-Scheepers, C., Jarzyna, M. A., Jennings, S., ... Williams, S. E. (2017). Biodiversity redistribution under climate change: Impacts on ecosystems and human well-being. *Science*, *355*, eaai9214–11. https://doi.org/10.1126/science.aai9214.

Rehm, E. M., & Feeley, K. J. (2015). The inability of tropical cloud forest species to invade grasslands above treeline during climate change: potential explanations and consequences. *Ecography*, *38*, 1167–1175. https://doi.org/10.1111/ecog.01050.

Reside, A. E., Butt, N., & Adams, V. M. (2018). Adapting systematic conservation planning for climate change. *Biodiversity and Conservation*, *27*, 1–29. https://doi.org/10.1007/s10531-017-1442-5.

Root, T., Price, J., Hall, K., Schneider, S., Rosenzweig, C., & Pounds, J. (2003). Fingerprints of global warming on wild animals and plants. *Nature*, *421*, 57–60. https://doi.org/10.1038/nature01333

Sanderson, B. M., Knutti, R., & Caldwell, P. (2015). A representative democracy to reduce interdependency in a multimodel ensemble. *Journal of Climate*, *28*, 5171–5194. https://doi.org/10.1175/JCLI-D-14-00362.1.

Saxon, E. (2008). Noah's Parks: A partial antidote to the Anthropocene extinction event. *Biodiversity*, *9*, 5–10. https://doi.org/10.1080/14888386.2008.9712901.

Scheffers, B. R., De Meester, L., Bridge, T. C. L., Hoffmann, A. A., Pandolfi, J. M., Corlett, R. T., Butchart, S. H. M., Pearce-Kelly, P., Kovacs, K. M., Dudgeon, D., Pacifici, M., Rondinini, C., Foden, W. B., Martin, T. G., Mora, C., Bickford, D., & Watson, J. E. M. (2016). The broad footprint of climate change from genes to biomes to people. *Science*, *354*, aaf7671–13. https://doi.org/10.1126/science.aaf7671

Seddon, A. W. R., Macias-Fauria, M., Long, P. R., Benz, D., & Willis, K. J. (2016). Sensitivity of global terrestrial ecosystems to climate variability. *Nature*, *531*, 229–232. https://doi.org/10.1038/nature16986

Sheridan, J. A., & Bickford, D. (2011). Shrinking body size as an ecological response to climate change. *Nature Climate Change*, *1*, 401–406. https://doi.org/10.1038/nclimate1259.

Sinclair, A. R. E., Mduma, S. A. R., Hopcraft, J. G. C., Fryxell, J. M., Hilborn, R., & Thirgood, S. (2007). Long-term ecosystem dynamics in the Serengeti: Lessons for conservation. *Conservation Biology*, *21*, 580–590. https://doi.org/10.1111/j.1523-1739.2007.00699.x

Sisneros, R., Huang, J., Ostrouchov, G., & Hoffman, F. (2011). Visualizing life zone boundary sensitivities across climate models and temporal spans. *Procedia Computer Science*, *4*, 1582–1591. https://doi.org/10.1016/j.procs.2011.04.171

Smith, J. R., Letten, A. D., Ke, P.-J., Anderson, C. B., Hendershot, J. N., Dhami, M. K., Dlott, G. A., Grainger, T. N., Howard, M. E., Morrison, B. M. L., Routh, D., San Juan, P. A., Mooney, H. A., Mordecai, E. A., Crowther, T. W., & Daily, G. C. (2018). A global test of ecoregions. *Nature Ecology & Evolution*, *2*, 1889–1896. https://doi.org/10.1038/s41559-018-0709-x

Smithers, J., & Smit, B. (1997). Human adaptation to climatic variability and change. *Global Environmental Change*, *7*, 129–146. https://doi.org/10.1016/S0959-3780(97)00003-4

Tatli, H., & Dalfes, H. N. (2015). Defining Holdridge's life zones over Turkey. *International Journal of Climatology*, *36*, 3864–3872. https://doi.org/10.1002/joc.4600

Tilman, D., Balzer, C., Hill, J., & Zimmermann, N. E. (2011). Global food demand and the sustainable intensification of agriculture. *Proceedings of the National Academy of Sciences USA*, *108*, 20260–20264. https://doi.org/10.1073/pnas.1116437108

Vitousek, P. M., Mooney, H. A., Lubchenco, J., & Melillo, J. M. (1997). Human Domination of Earth's Ecosystems. *Science*, *277*, 494–499. https://doi.org/10.1126/science.277.5325.494

Ward, M., Saura, S., Williams, B., Ramírez-Delgado, J. P., Arafeh-Dalmau, N., Allan, J. R., Venter, O., Dubois, G., & Watson, J. E. M. (2020a). Just ten percent of the global terrestrial protected area network is structurally connected via intact land. *Nature Communications*, *11*, 4563. https://doi.org/10.1038/s41467-020-18457-x

Ward, M., Tulloch, A. I. T., Radford, J. Q., Williams, B. A., Reside, A. E., Macdonald, S. L., Mayfield, H. J., Maron, M., Possingham, H. P., Vine, S. J., O'Connor, J. L., Massingham, E. J., Greenville, A. C., Woinarski, J. C. Z., Garnett, S. T., Lintermans, M., Scheele, B. C., Carwardine, J., Nimmo, D. G., ... Watson, J. E. M. (2020b). Impact of 2019–2020 mega-fires on Australian fauna habitat. *Nature Ecology & Evolution*, *4*, 1321–1326. https://doi.org/10.1038/s41559-020-1251-1.

Watson, J. E. M., Iwamura, T., & Butt, N. (2013). Mapping vulnerability and conservation adaptation strategies under climate change. *Nature Climate Change*, *3*, 989–994. https://doi.org/10.1038/nclimate2007

Williams, J., & Jackson, S. (2007). Novel climates, no-analog communities, and ecological surprises. *Frontiers in Ecology and the Environment*, *5*, 475–482. https://doi.org/10.1890/070037.

Woodward, F. I., Lomas, M. R., & Kelly, C. K. (2004). Global climate and the distribution of plant biomes. *Philosophical Transactions of the Royal Society B: Biological Sciences*, *359*, 1465–1476. https://doi.org/10.1098/rstb.2004.1525

Xu, C., Kohler, T. A., Lenton, T. M., Svenning, J.-C., & Scheffer, M. (2020). Future of the human climate niche. *Proceedings of the National Academy of Sciences USA*, *117*, 11350–11355. https://doi.org/10.1073/pnas.1910114117

Xu, J., Grumbine, R. E., Shrestha, A., Eriksson, M., Yang, X., Wang, Y., & Wilkes, A. (2009). The Melting Himalayas: Cascading Effects of Climate Change on Water, Biodiversity, and Livelihoods. *Conservation Biology*, *23*, 520–530. https://doi.org/10.1111/j.1523-1739.2009.01237.x

Zabel, F., Putzenlechner, B., & Mauser, W. (2014). Global agricultural land resources—A high resolution suitability evaluation and its perspectives until 2100 under climate change conditions. *PLoS One*, *9*, e107522. https://doi.org/10.1371/journal.pone.0107522

Zomer, R. J., Trabucco, A., Bossio, D. A., & Verchot, L. V. (2008). Climate change mitigation: A spatial analysis of global land suitability for

clean development mechanism afforestation and reforestation. *Agriculture Ecosystems & Environment*, *126*, 67–80. https://doi.org/10.1016/j.agee.2008.01.014

SUPPORTING INFORMATION

Additional supporting information may be found in the online version of the article at the publisher's website.